

# Wet Compression Performance of a Transonic Compressor Rotor at its Near Stall Point

Huaifeng Yang<sup>1</sup>, Qun Zheng<sup>1\*</sup>, Mingcong Luo<sup>1</sup>, Lanxin Sun<sup>1</sup> and Rakesh Bhargava<sup>2</sup>

1. College of Power and Energy Engineering, Harbin Engineering University, Harbin 150001, China

2. Foster Wheeler USA Corp, Houston TX 77052-3495, USA

**Abstract:** In order to study the effects of wet compression on a transonic compressor, a full 3-D steady numerical simulation was carried out under varying conditions. Different injected water flow rates and droplet diameters were considered. The effect of wet compression on the shock, separated flow, pressure ratio, and efficiency was investigated. Additionally, the effect of wet compression on the tip clearance when the compressor runs in the near-stall and stall situations was emphasized. Analysis of the results shows that the range of stable operation is extended, and that the pressure ratio and inlet air flow rate are also increased at the near-stall point. In addition, it seems that there is an optimum size of the droplet diameter.

**Keywords:** wet compression; two-phase flow; stall boundary; transonic compressor

**Article ID:** 1671-9433(2011)01-0049-14

## 1 Introduction

With the modern axial compressor developing into high stage pressure ratio, high blade load and high tip velocity, the problem of stable operation becomes very important. Generally, the high stage pressure ratio or high blade load will result in a transonic stage, especially the front stage of a compressor. The unstable operation of the compressor may lead to the deteriorating of the performance, even the engine broken. It is always try to find a way to extend the range of stable operation, to keep the high efficiency at the same time, and to make the compressor work safely and economically. There are several techniques available for extending the range of stable operation, such as rotating the stator vane, extracting compressed air in the middle stage and casing treatment (Chaker and Meher-Homji, 2008). Air injection in the blade tip area of a compressor is one of the techniques to improve the stable operation of compressor, which has been investigated by Sven-Jürgen *et al.* (2009). Water injection could be another way to help to extend the stable operating range of compressor. That is what we want to investigate in this paper.

Wet compression or water injection in the compressor was applied initially for increasing the gas turbine output power when the ambient temperature rises. This technology will decrease the compression power and increases the efficiency of compressor theoretically. And it has been successfully applied in industry for business operation. It is estimated that there are over 1000 gas turbines that use high pressure

fogging or overspray worldwide (Bhargava *et al.*, 2005; Bianchi *et al.*, 2007). However, this technology has not been fully understood in theory and its potentials to maintain the operating stability of the compressor. Some analytical and experimental studies have been made in recent years (März *et al.*, 2001; Härtel and Pfeiffer, 2003; Song *et al.*, 2005). Actually, the possibility of wet compression to suppress the unstable operation of compressor has been researched in several papers (Wang *et al.*, 2002; Wang *et al.*, 2003; Li and Zheng, 2004). Based on the Moore-Greitzer model, Wang, Li and Zheng have developed a wet compression M-G model. The simulation results indicate that under certain conditions, the wet compression can eliminate the stall and surge to some extent and extend the range of stable operation. Wang has also investigated wet compression to extend the range of stable operation of an aero-engine (Chaker *et al.*, 2003). Day and Williams have done an experiment of rain ingestion in an axial flow compressor. The experiment of rain ingestion results in a decreasing of the compressor efficiency and the stability (Day *et al.*, 2005). The diameter of droplet in Day's experiment is above 50-70  $\mu\text{m}$  and the amount of flow rate is heavy to simulate the rain ingestion. The big droplets in their experiment are perturbations to the compressor flow, when the droplets flow into the compressor, they will move to the endwalls and block the flow channel. However, they could not to measure the flows details in the compressor cascade. So it is deserved to investigate the flow fields in the compressor by CFD to evaluate the water injection effects on the compressor performances, especially the supersonic compressor stage.

CFD has been used to simulate the two phase flows in the wet compressor cascades (Shao *et al.*, 2006; Bianchi *et al.*, 2007). Sun and Zheng (2008) indicated the water droplets' evaporative cooling can suppress the separated flows at off design conditions (Sun and Zheng, 2008). The compressor

---

**Received date:** 2009-12-01.

**Foundation item:** Supported by the National Natural Science Foundation of China under Grant No.50776021.

\*Corresponding author Email: zhengqun@hrbeu.edu.cn

© Harbin Engineering University and Springer-Verlag Berlin Heidelberg 2011

cascades that are simulated in these CFD studies are subsonic cascades, and what they investigated is not a front stage, which means a higher inlet pressure and higher inlet temperature than those of a front stage. In this study, we try to focus on the two phase flow fields of a transonic rotor with wet compression. The effects of wet compression on the rotor performance are investigated, and we pay special attentions to the shockwaves and stalls after the water is injected into the flow channels of the transonic rotor.

## 2 The transonic compressor rotor

Rotor 37 was designed and tested by NASA Glenn Research Center in the 1970s, which is one of the four high pressure compressor rotors that the American Society of Mechanical Engineers (ASME) used it as a “blind” test case for the CFD codes to evaluate the simulation ability of those different numerical codes. The experimental data and test results were reported by ASME in the next year. And then this compressor rotor became one of standard test cases in the turbomachinery area (Shibata *et al.*, 2008). The basic design parameters are shown in Table 1. Detailed design parameters and experimental data could be found in Moore (1978). The compressor geometry model is shown in Fig.1.

**Table1 Rotor 37 design parameters**

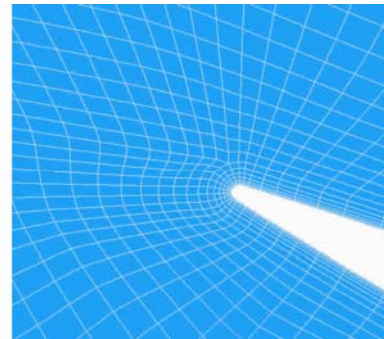
Parameter	Value
Design flow rate $/(kg \cdot s^{-1})$	20.19
Pressure ratio	2.106
Rotational speed $/(r \cdot min^{-1})$	17 188.2
Number of blades	36
Tip clearance /mm	0.356
Tip solidity	1.288
Aspect ratio	1.19
Shroud hub ratio	0.70
Tip speed $/(m \cdot s^{-1})$	454.14



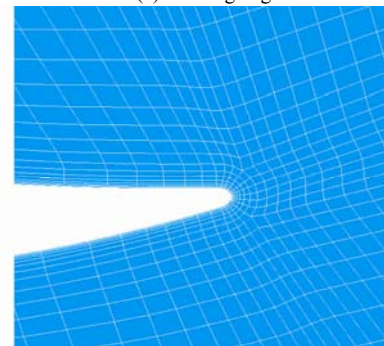
**Fig.1 The compressor rotor geometry model**

In this paper, we choose the  $\kappa$ - $\epsilon$  model as the turbulence model, and use the commercial fluid software CFX has been used. TurboGrid software was used to generate meshes in all computational domains. H-type grids were used at the leading edge, trail edge, tip clearance and the main passage. O-type grid was used around the blade. The grid distribution is shown in Fig.2. In order to check for grid dependency, we have computed the rotor flow fields with 250 000 and 500 000 grid nodes respectively, the results present little differences, so the

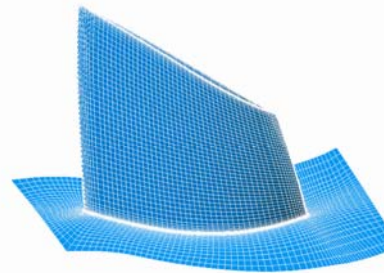
number of total grids number is chosen as 250 000. The inlet boundary conditions are total pressure and total temperature. At the outlet, static pressure is specified. The blade, hub and casing walls are adiabatic wall and no slip conditions applied. When water droplets are sprayed into the rotor flow field, it is assumed a even distribution at the inlet. If the droplets attack the walls, it is assumed an elastic collision conditions as used in CFX. The particle transport model was used for the disperse phase.



(a) Leading edge



(b) Trailing edge

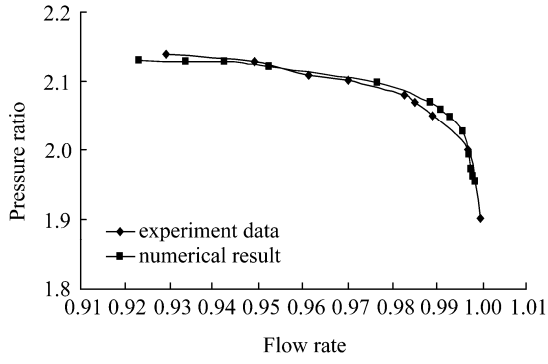


(c) Rotor

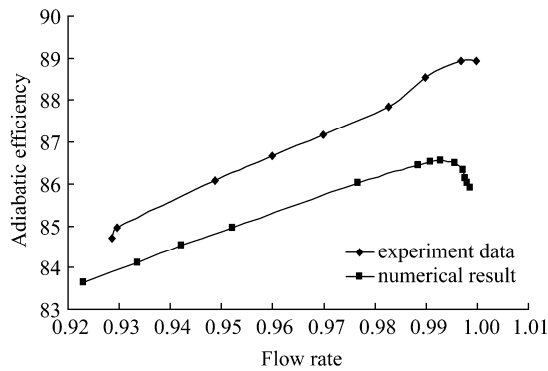


(d) Shroud tip

**Fig.2 The mesh distribution**

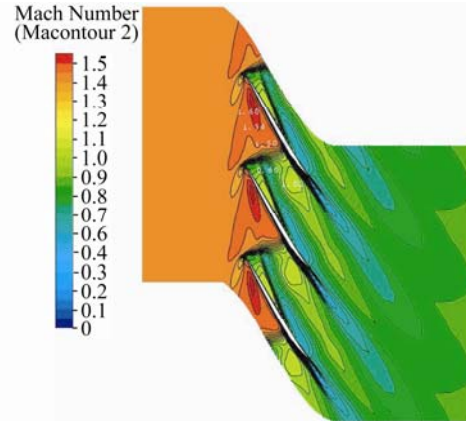


(a) The relationship of flow rate and pressure ratio

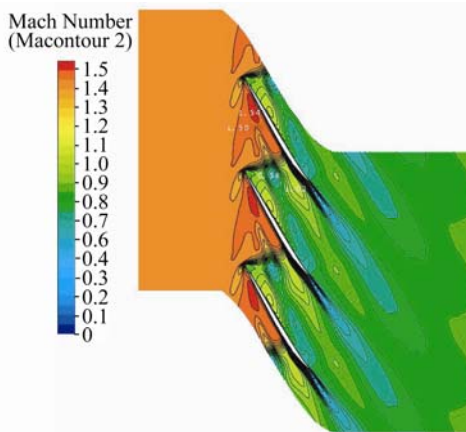


(b) The relationship of flow rate and efficiency

**Fig.3 Numerical results compared with experimental data**

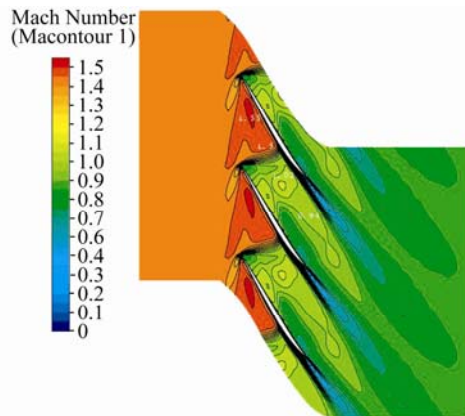


(c) Dry 97% span

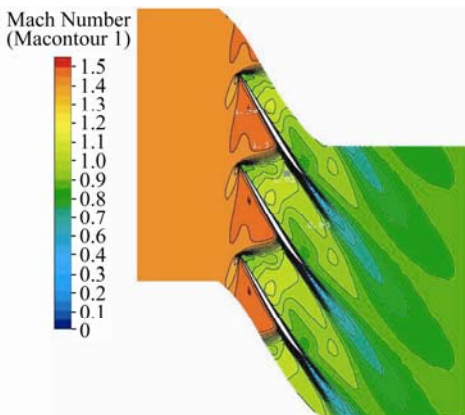


(d) Wet 97% span

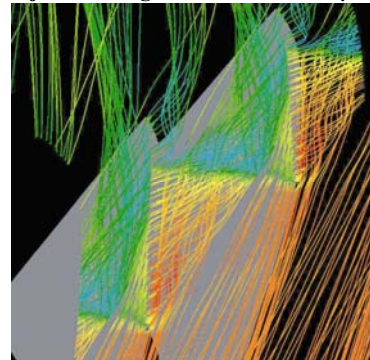
**Fig.4 Mach number contour at back pressure 125 534 Pa, water injected 180 g/s, and diameter 5 μm**



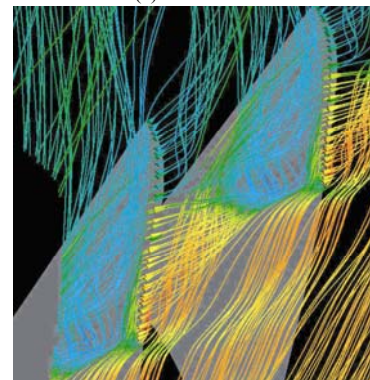
(a) Dry 95% span



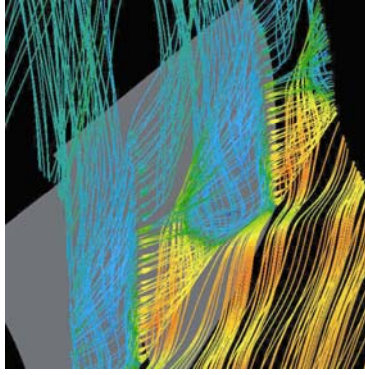
(b) Wet 95% span



(a) 125 534 Pa



(b) 134 534 Pa



(c) 135 534 Pa

**Fig. 5 Streamlines in the clearance under different static pressures (125 534, 134 534 and 135 534 Pa)**

### 3 Numerical simulations and results

Calculation starts firstly from the outlet static pressure 115534Pa with no water droplets injected. The calculated flow rate is close to the measured maximum flow rate under this condition. Then the outlet pressure is increased step by step. The step size is big at first, it could get a maximum efficiency, then the step size becomes small until 100 Pa when it is near stall. When calculating the wet compression, we start from the same pressure as the dry compression. The rule to judge the flow unstable is: the compressor inlet and outlet flow rate and efficiency decrease continually, when the calculated step increases (Fabrizzi *et al.*, 2009).

**Table 2 Calculated results at different outlet static pressures**

Items	125 534 Pa			134 534 Pa			135 534 Pa		
	Inlet flow rate/ (kg·s <sup>-1</sup> )	Pressure ratio	Efficiency/ %	Inlet flow rate/ (kg·s <sup>-1</sup> )	Pressure ratio	Efficiency/ %	Inlet flow rate/ (kg·s <sup>-1</sup> )	Pressure ratio	Efficiency/ %
Dry	20.74	2.059	86.20	19.32	2.130	83.12	18.82	2.130	81.95
72 g/s 1 μm	20.56	2.053	86.08	19.31	2.130	82.81	18.86	2.133	81.69
72 g/s 5 μm	20.61	2.051	86.02	19.48	2.133	83.34	19.09	2.138	82.35
72 g/s 10 μm	20.61	2.051	86.26	19.48	2.133	83.37	19.04	2.137	82.14
180 g/s 1 μm	20.50	2.053	84.95	19.21	2.127	81.60	—	—	—
180 g/s 5 μm	20.61	2.048	85.85	19.63	2.135	83.59	19.29	2.141	82.63
180 g/s 10 μm	20.62	2.048	86.14	19.62	2.134	83.64	19.26	2.139	82.66
324 g/s 1 μm	20.45	2.0518	83.22	19.21	2.1282	79.97	—	—	—
324 g/s 5 μm	20.60	2.0457	85.40	19.76	2.1364	83.19	19.49	2.1431	82.64
324 g/s 10 μm	20.63	2.0448	85.97	19.77	2.1346	83.89	19.48	2.1406	83.07
432 g/s 1 μm	20.43	2.0496	82.82	19.26	2.1292	79.83	—	—	—
432 g/s 5 μm	20.59	2.0431	85.14	19.84	2.1342	83.15	19.61	2.1422	82.34
432 g/s 10 μm	20.64	2.0419	85.86	19.86	2.1344	84.05	19.62	2.1411	83.36

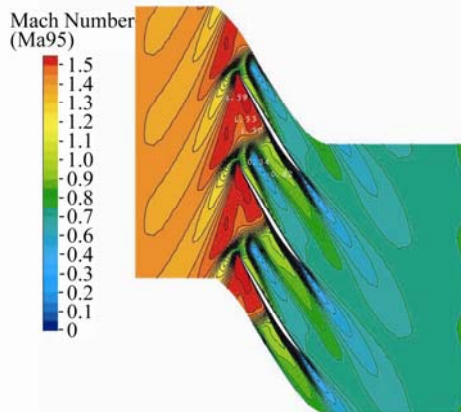
#### 3.1 Rotor performances of dry compression

The dry compression performance of the pressure ratio and efficiency are shown in Fig.3. The abscissa is flow rate which is normalized by the maximum flow rate 20.93 kg/s. As shown in Fig.3, the calculated pressure ratios are close to the experimental data, but the calculated efficiencies are lower than experiment data about 2%–3%. These results are similar to other researcher's results in (Ulrichs and Joos, 2006). In addition, the stall flow is about 0.923, which is lower than experimental data.

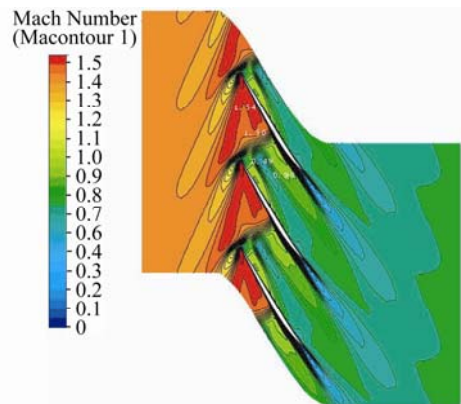
#### 3.2 Comparisons of wet and dry compressions

In this section, wet compressions are compared with dry compression under different back pressures (all the pressure is absolute pressure in this paper) 125 534, 134 534 and 135534Pa respectively. The fogging flow rate is 0.18 kg/s and the diameter of water droplet is 5 μm. When the pressure is 125 534 Pa, the compressor rotor runs at designed point with the inlet flow rate of 20.74 kg/s and pressure ratio 2.059. When the pressure is 134 534 Pa, the compressor rotor runs near stall with inlet flow rate of 19.32 kg/s and pressure ratio 2.13. When the pressure is 135 534 Pa, the compressor rotor

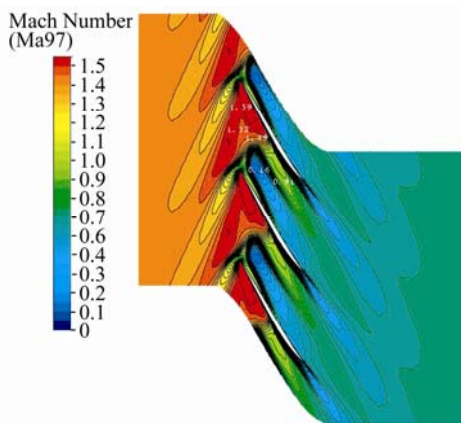
runs at the stall with inlet flow rate of 18.82 kg/s and pressure ratio of 2.13. The Mach numbers at 95% span of the pressure 125 534 Pa of dry and wet cases are shown in Fig.4(a) and Fig.4(b). After water injected, the Mach number changes a little and the shape is much the same. But in 97% span, the fogging changes the shape of the shock. The smallest Mach number decreases from 0.6 to 0.58. And the low Mach number area increases and moves into centre. The inlet flow rate decreases after fogging (Table 2). The dry inlet flow rate is 20.74 kg/s, but it decreases to 20.61 kg/s with fogging.



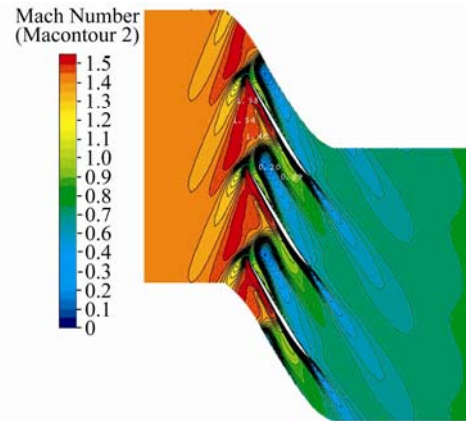
(a) Dry 95% span



(b) Wet 95% span



(c) Dry 97% span



(d) Wet 97% span

**Fig.6 Mach number contours, in which static back pressure is 134 534 Pa, water injected 180 g/s, and diameter 5 μm**

The results indicate that the tip leakage vortex is the key to the Rotor 37 (Hofman and Ballmann, 2002; Furukawa *et al.*, 1998). Fig.5 shows that the streamline in the tip clearance changes under different pressures. In Fig.5(b), the compressor is running near stall, we can see that the leakage streamline forms a low speed area in the passage, which leads to the inlet flow and efficiency decrease. With the pressure increasing this area becomes strong and big, so the compressor runs into stall. In Fig.5(c), the pressure is 135 534 Pa. Compared with Fig.5(b), we find the low speed area is enlarged and there is a vortex. In Fig.6, the compressor is running near stall at 134534 Pa, compared with dry compression, the smallest Mach number increases from 0.34 to 0.49 at 95% span, and from 0.16 to 0.20 at 97% span. And the low speed area reduces. These indicate that fogging increases the minimum Mach number and the inlet flow rate (Table 2). When pressure is 135 534 Pa, the minimum Mach number increases from 0.17 to 0.29 at 95% span, and from 0.05 to 0.14 at 97% span (Fig.7), and the low speed area also reduces. In Fig.8(a), there is a circumfluence at 97% span in the dry compression. But fogging eliminates the circumfluence in Fig.8(b) and the streamlines come back normally. This indicates that the compressor may come back from stall and runs stable with wet compression. The wet compression also changes the temperature distributions comparing with those of dry compression. The dark red area, which represents the high temperature, decreases with fogging as shown in Fig.9. At the same time, the fogging also decreases the total pressure loss as shown in Fig.10.

From the flow rates and pressure ratios curves, we find that the inlet flow rate and the pressure ratio increase in Fig.11 (except for 1 μm). In addition, when the fogging rate is 180g/s and the droplet diameter is 5 μm, the inlet flow rate decreases to 19.02 kg/s at 135 534 Pa and then goes into stall. Compared with the dry compression, the stable operation range enlarged. In order to compare the effects under all fogging conditions, we analyzed the rotor performance at different fogging rates and droplet diameters.

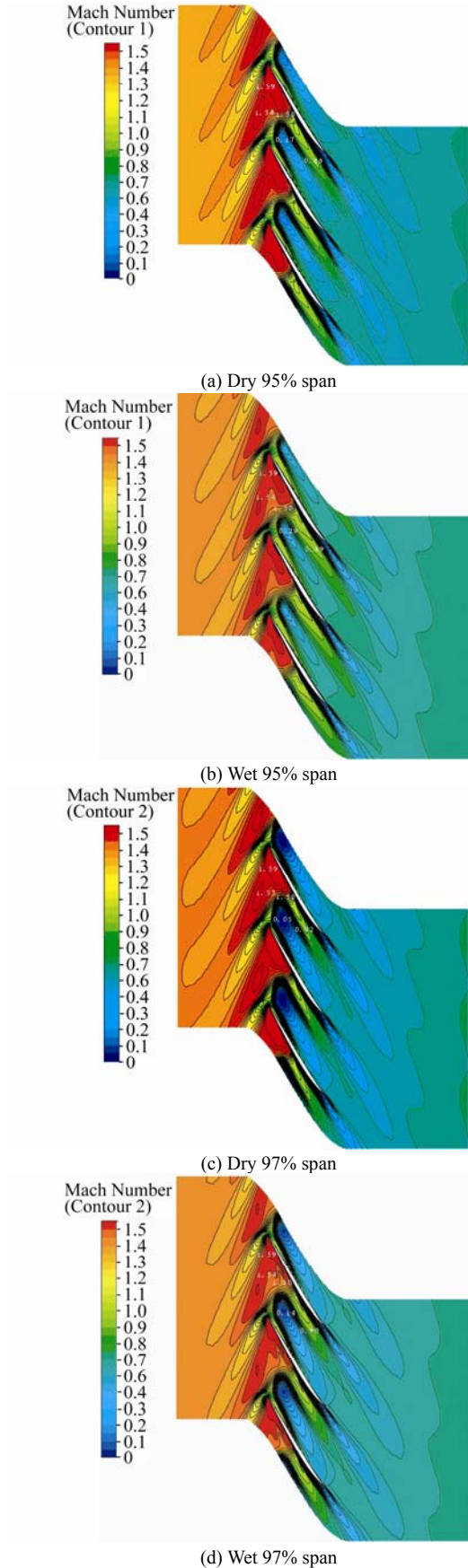


Fig.7 Mach number contours, in which static back pressure is 135534 Pa, water injected 180 g/s, and diameter 5  $\mu\text{m}$

Compared the inlet flow rates under three different pressure in Table 2, we find that the fogging decreases the inlet flow rates when the compressor runs near the designed point and only when the compressor runs near stall could the fogging increase the inlet flow rates. The reason is that the fogging worsens the flow fields when the compressor runs near designed point, but the fogging benefits the flow fields when the compressor runs near stall. The particle of 1  $\mu\text{m}$  can not increase the inlet flow rate as shown in Fig.11.

Figs.12 and 13 show the wet performance characteristic lines, in which water droplet diameter is 1  $\mu\text{m}$ . These lines are generally lower than the dry characteristic line at the same inlet flow rate. But when the water droplet diameter is 5  $\mu\text{m}$  and 10  $\mu\text{m}$ , the wet performance characteristic lines are higher than the dry characteristic line, if the inlet flow rates are lower than some value. Compared the two figures, we can find that the stall pressure ratio is higher if more water droplets are injected in the case of 5  $\mu\text{m}$  and 10  $\mu\text{m}$ , and we find the 5  $\mu\text{m}$  water droplet is the best particle diameter. It is of the highest stall pressure ratio and the widest range of stable operation at any fogging rate.

The wet compression efficiency can be divided into two parts, namely dry air compression work and water vapor compression work. To simplify the computation, we can assume that all gas is compressed from  $P_{t1}$  to  $P_{t2}$ . So the wet compression efficiency is given by

$$\eta_w = \frac{W_{wi}}{W_w} \quad (1)$$

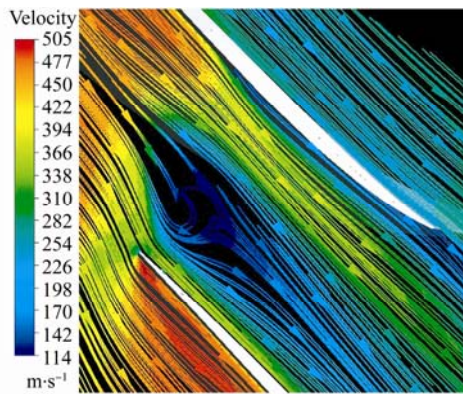
$$W_{wi} = (W_a + fW_v)/(1 + f) \quad (2)$$

$$W_w = \omega M_t / m_{\text{out}} \quad (3)$$

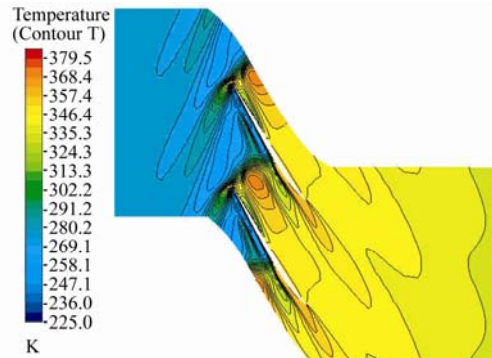
$$W_a = (h_{t2,i} - h_{t1})_a = C_{pa} T_{t1} \left[ \left( \frac{P_{t2}}{P_{t1}} \right)^{\frac{\gamma_a - 1}{\gamma_a}} - 1 \right] \quad (4)$$

$$W_v = (h_{t2,i} - h_{t1})_v = C_{pv} T_{t1} \left[ \left( \frac{P_{t2}}{P_{t1}} \right)^{\frac{\gamma_v - 1}{\gamma_v}} - 1 \right] \quad (5)$$

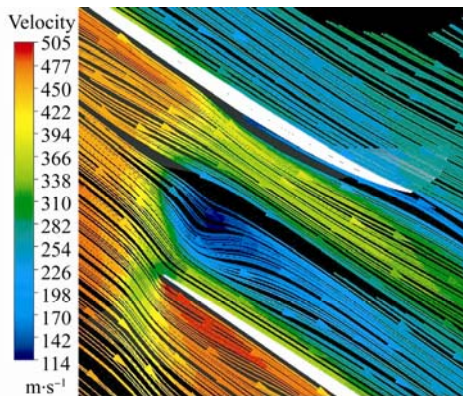
where  $W_{wi}$ ,  $W_w$  are isentropic and actual specific work of wet compression, respectively (J/kg);  $W_a$ ,  $W_v$  the specific compression work of gas and vapor component, respectively (J/kg);  $f$  the outlet steam-to-air ratio;  $h$  the Enthalpy (J/kg); and  $\omega$  the rotation speed (rad/s).  $M_t$  the torque on the rotor (N·m), which is given by the program directly;  $m_{\text{out}}$  stage outlet mass flowrate (kg/s);  $C_p$  the specific heat (J/kg·K), 1005 and 4199.2 for air and water vapor, respectively;  $\gamma$  the ratio of specific heat, 1.4 and 1.01 for air and water vapor, respectively;  $a$ ,  $v$  the subscript air and outlet vapor component, respectively;  $t$  the subscript total; 1, 2 the subscript stage inlet and outlet, respectively.



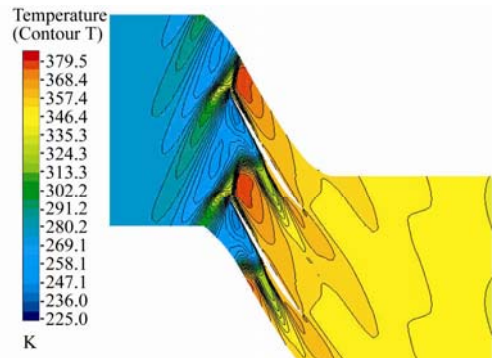
(a) Dry 97% span



(b) Wet 180 g/s 5 μm 135 534 Pa



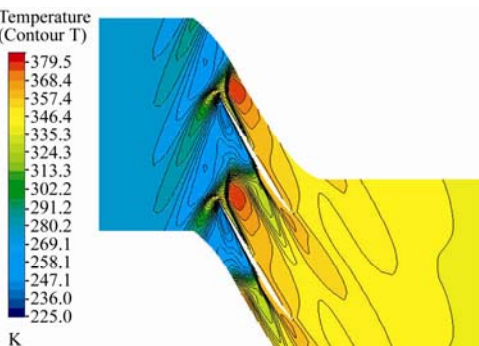
(b) Wet 97% span



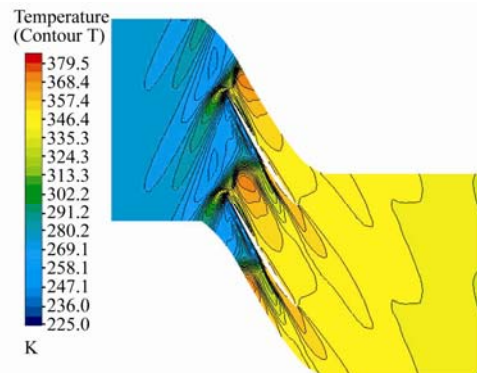
(c) Dry 135 534 Pa

**Fig.8 Streamlines under static pressure 135 534 Pa, water injected 180 g/s, diameter 5 μm**

According to the efficiency definition, we have drawn Figs.14 and 15 based on the computational results. The wet compression efficiency is lower than dry efficiency at all conditions except for some special flow rate like 0.072 kg/s. Especially, for the 1 μm particle, the efficiency decreases when the fogging rate increases. The main reason is that the inlet temperature is lower, the temperature rising is small and the staying time in the passage is also short which lead to the benefit for droplet evaporation is very small. On the contrary, the fogging has adverse effects on the flow fields, which leads to decreasing efficiency. For example, with the 1 μm diameter and the fogging rate of 0.18 kg/s at 135 534 Pa, the outlet temperature decreases less than 1 K compared with dry compression.

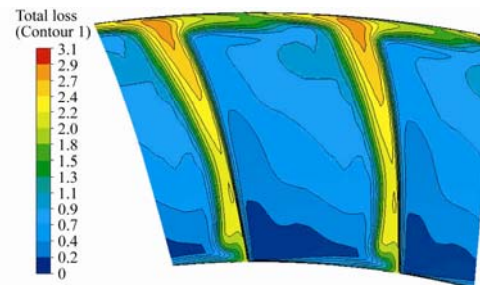


(a) Dry 135 534 Pa

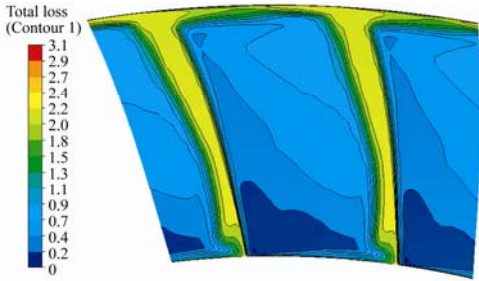


(d) Wet 180 g/s 5 μm 135 534 Pa

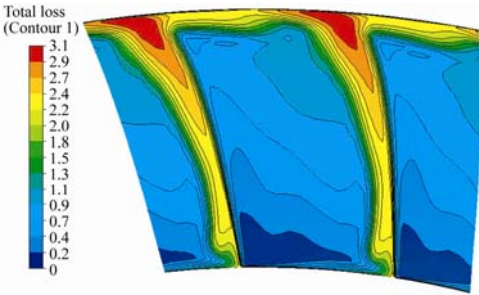
**Fig.9 Temperature contours at 97% span**



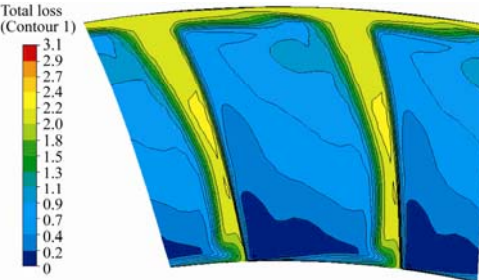
(a) Dry 135 534 Pa



(b) Wet 180 g/s 5 μm 134534 Pa

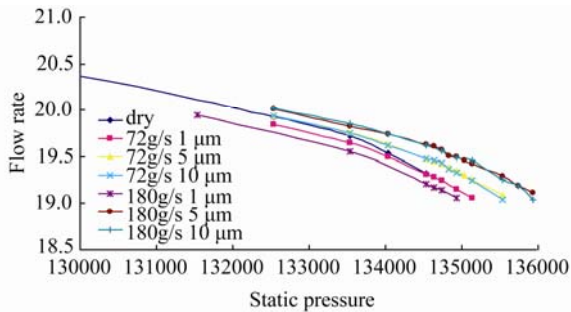


(c) Dry 135534 Pa

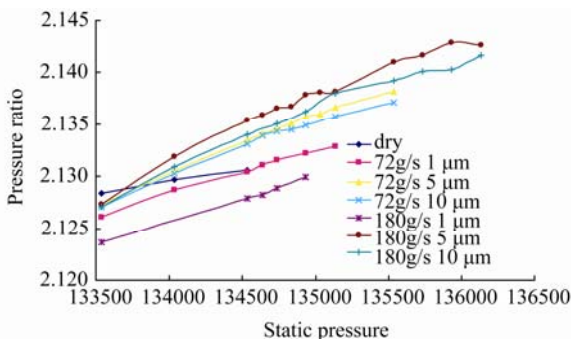


(d) Wet 180 g/s 5 μm 134534 Pa

Fig.10 Total pressure losses behind the trailing edge

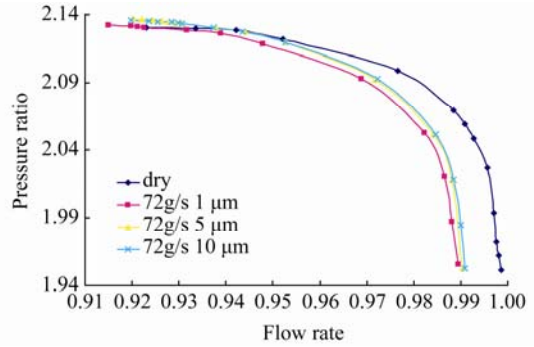


(a) The relationship of static pressure with inlet flow rate

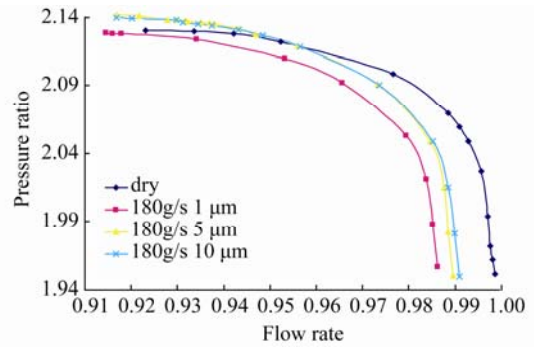


(b) The relationship of static pressure with total pressure ratio

Fig.11 Comparison of results of the wet characteristic line with dry case

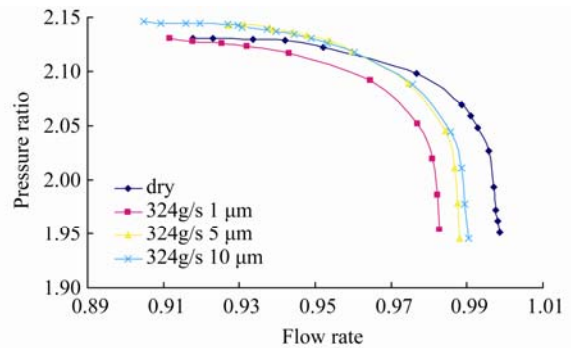


(a) 72 g/s

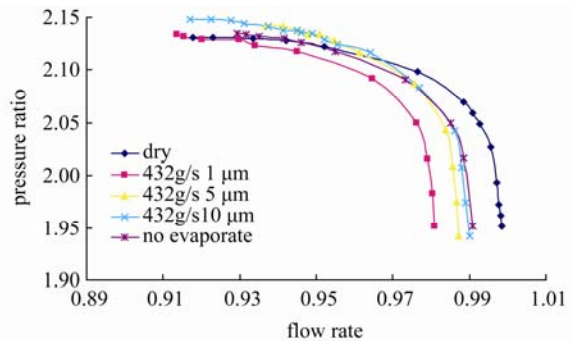


(b) 180 g/s

Fig.12 The relationship of inlet flow rate with total pressure ratio

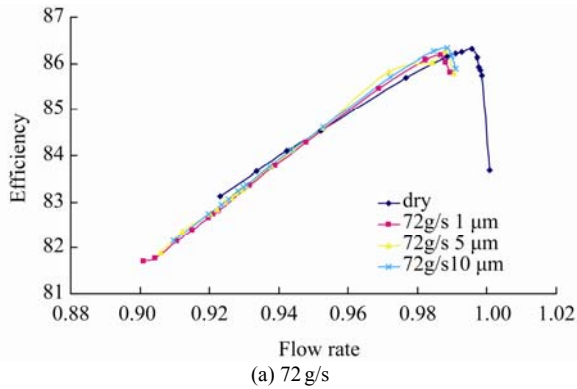


(a) 324 g/s

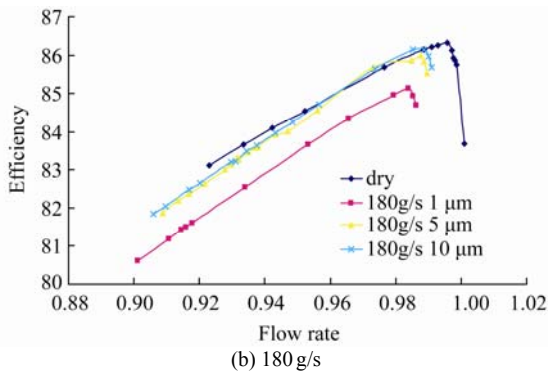


(b) 432 g/s

Fig.13 The relationship of inlet flow rate with total pressure ratio

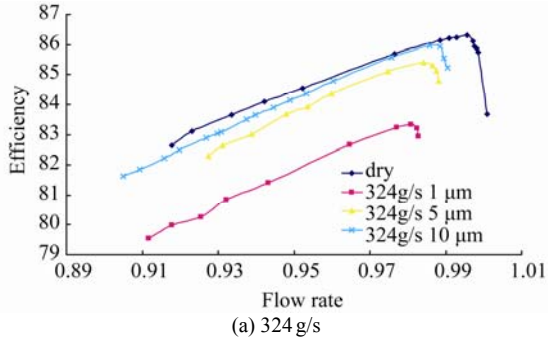


(a) 72 g/s

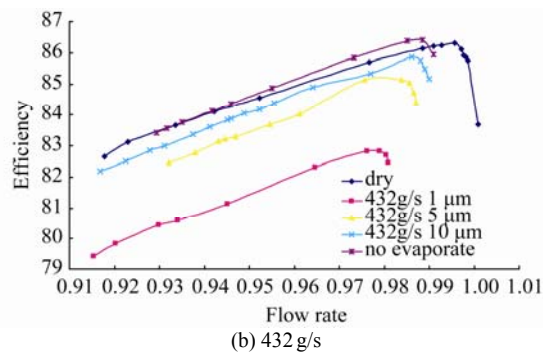


(b) 180 g/s

Fig.14 the relationship of inlet flow rate with efficiency



(a) 324 g/s



(b) 432 g/s

Fig.15 The relationship of inlet flow rate with efficiency

From above figures and analyses, we find that the range of stable operation could extend with fogging, but the efficiency will decrease especially for the heavy fogging. This phenomenon is observed for the single transonic compressor rotor that is different from the general wet compression

phenomena for multi stage compressors. The experiment by Day *et al.* (2005) for rain ingestion in axial flow compressor had the similar decreasing effect of the compressor efficiency and stability. the wet compression experiment of a single stage compressor by Gong and Nie had the similar results. But the diameter of droplet in Day’s experiment was about 50-70  $\mu\text{m}$ , which could not flow with air. In Gong’s paper, it did not provide the diameter of droplet.

### 3.3 The reason for stable operation range extension

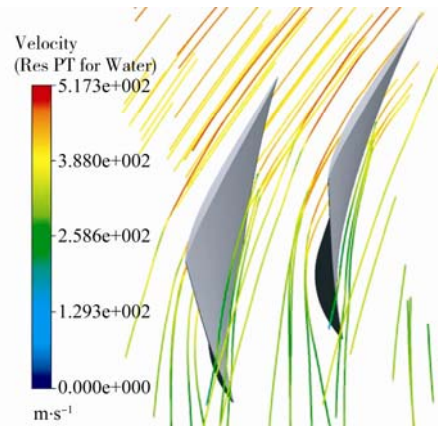
The stall of Rotor 37 was caused by the leakage vortex. This point will be discussed further in this paper, which includes wet compression effects:

1) When injected water particle diameter is 1  $\mu\text{m}$ , the fogging decreases the inlet flow rate and the pressure ratio at any fogging rate.

2) When the particle diameter is 5  $\mu\text{m}$  and 10  $\mu\text{m}$ , the pressure ratio and inlet flow rate are higher than dry compression only when the compressor runs near stall. The fogging has extended the range of stable operation and the 5  $\mu\text{m}$  particle can provide higher pressure ratio than that of 10  $\mu\text{m}$  as shown in Fig.7. The 5  $\mu\text{m}$  water particle injection increases the inlet flow rate than that of 10  $\mu\text{m}$ . If compared with 1  $\mu\text{m}$  case, there will be an optimum value of the droplet diameter.

3) From the pressure-inlet flow rate curve, we find that the 1  $\mu\text{m}$  particle can not increase inlet flow at the same pressure. When the diameter is 5  $\mu\text{m}$  and 10  $\mu\text{m}$ , the more the fogging rate increase, the bigger the inlet flow rate is.

We sum up two points about 1  $\mu\text{m}$ , 5  $\mu\text{m}$  of which the mass discrepancy is 125 times. It has been mentioned that the stall of Rotorn37 was caused by the leakage vortex which blocked the main passage flow. Although the three particles can flow with air (That has been shown in Fig.16), the mass of 1  $\mu\text{m}$  is too small. However, the mass of 5  $\mu\text{m}$  is relatively big in size and is of more momentum. So the velocity is also higher when it passes through the shock.



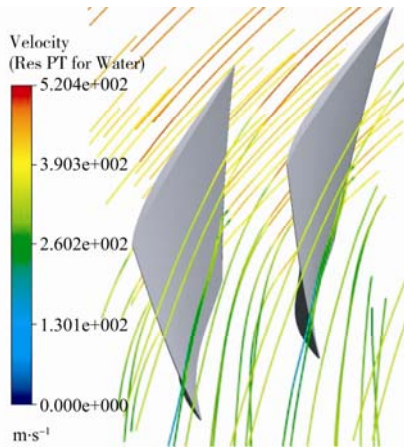


Fig.16 1  $\mu\text{m}$ , 5  $\mu\text{m}$  particle tracks

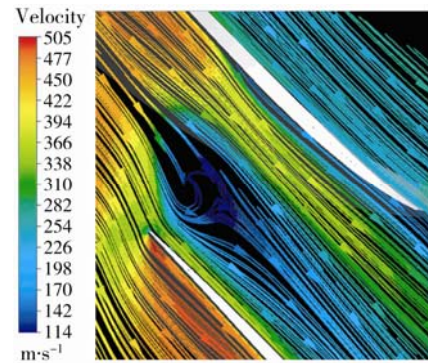
Therefore the relatively higher velocity particle can drive the low speed area which formed near the tip. The improved velocity also increases the inlet flow rate. This characteristic is shown in Fig.17. The fogging can not eliminate the vortex with 1  $\mu\text{m}$  and 5  $\mu\text{m}$  size when the flow rate is 0.072 kg/s. But the 10  $\mu\text{m}$  can eliminate the vortex at the same fogging rate. In addition, with the fogging flow rate increasing to 0.18kg/s, the 5  $\mu\text{m}$  will also eliminate the vortex in the clearance. In the computational process, the compressor stalled at 135 534 Pa with a fogging flow rate of 0.18 kg/s. So compared with 0.072 kg/s in Fig.17(b), we find that 1  $\mu\text{m}$  fogging can not eliminate the eddy even though the fogging rate increases because of its too small mass. The inlet flow rate and efficiency decreasing is caused by the block of stall region of dry compression. The big mass particle can drive the low speed air to decrease the extent of blocking and the efficiency and inlet flow rate increase at the same time. That is why the big particle evaporates little, but the efficiency is higher than those of small particles.

The effect of evaporation for small particle is better, but it can not eliminate the block, which locates in the main passage near tip. So the benefit of evaporation to improve the efficiency is called off by the block in the main passage near tip. Absolutely, the evaporation could improve the efficiency, especially with the high inlet temperature. Next we will discuss the momentum impact of water particle on the shock position and the flow separation.

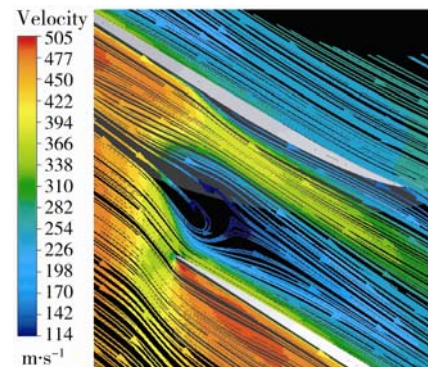
The effect of evaporation for small particle is better, but it can not eliminate the block, which locates in the main passage near tip. So the benefit of evaporation to improve the efficiency is called off by the block in the main passage near tip. Absolutely, the evaporation could improve the efficiency, especially with the high inlet temperature. Next we will discuss the momentum impact of water particle on the shock position and the flow separation.

From Fig.18, we also find that the shock position moves forward in the suction side, whatever 50% span or 90% span,

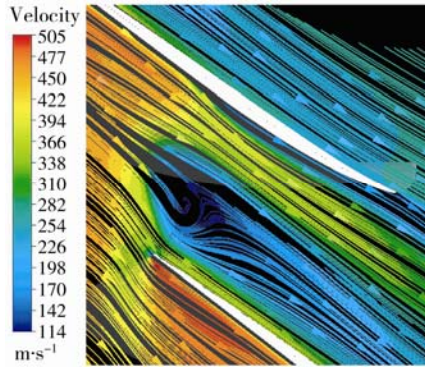
when the outlet pressure increases. The result of this move is the inlet flow rate decreasing. The nearer forward it moves, the little inlet flow rate is. In the case of wet compression, as shown in Fig.19, compared with the dry compression, the limiting streamlines on the rotor blade suction surfaces of wet compression show the changes of separated points. The fogging moves the point toward trailing edge, but it does not change the shock shape just as shown in Fig.20. The shock position moves just a little when the compressor runs at designed point in Figs.21(a) and (b). But it moves back some distance when the compressor runs near stall in Figs.21(c) and (d). It shows more distance when the compressor runs at 13534 Pa in Figs.21(e) and (f). From above we discussed, we know the shock position can impact the inlet flow rate. The nearer forward it moves, the little the inlet flow rate is. From the results that discussed in Fig.21, we know that the fogging makes the shock position move back. That means the fogging improves the inlet flow rate under the same pressure, which is similar to the above discussed result. In this paper, when the pressure reaches some value, the wet pressure ratio with 5  $\mu\text{m}$  and 10  $\mu\text{m}$  is higher than dry compression. This is similar with the characteristic line's change trend that was assumed by Wang *et al.* (2003). According to this change trend, they modified the wet compression M-G model and found that the wet compression can restrain the compression stall theoretically. So the calculated result in this paper consolidates their theory.



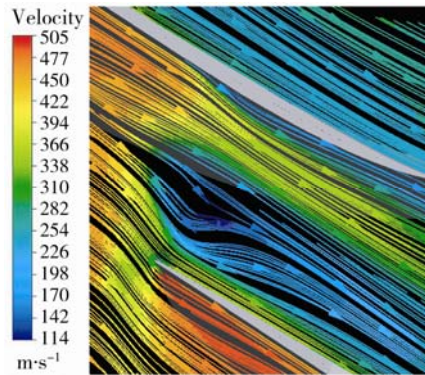
(a) Dry



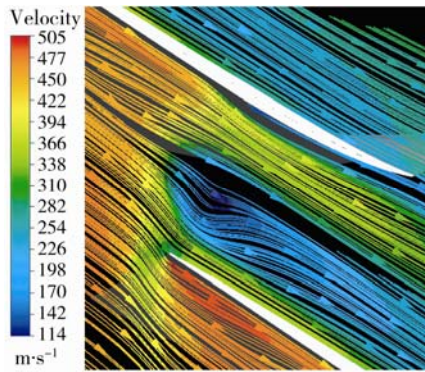
(b) 72 g/s 1  $\mu\text{m}$



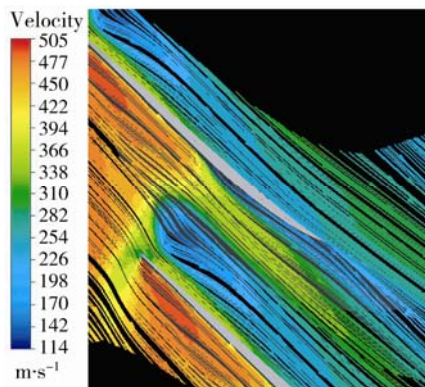
(c) 72 g/s 5 μm



(d) 72 g/s 10 μm

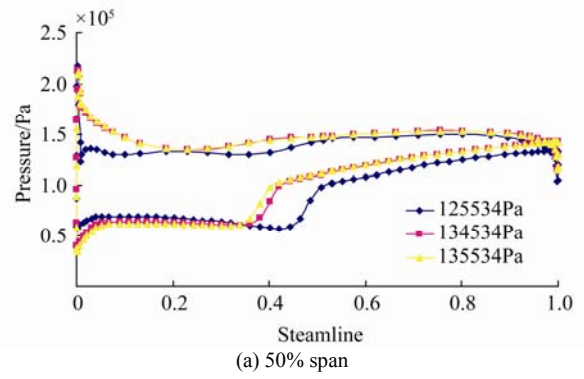


(e) 180 g/s 5 μm

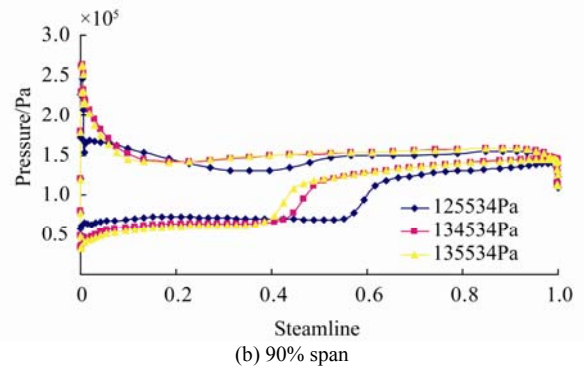


(f) 180 g/s 10 μm

Fig.17 Streamlines at 97% span under the pressure 135534 Pa

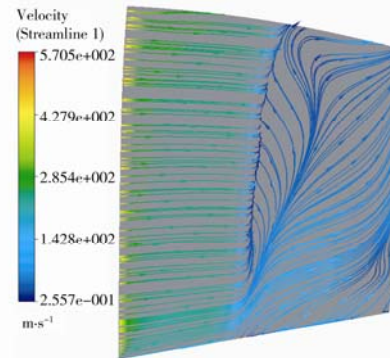


(a) 50% span

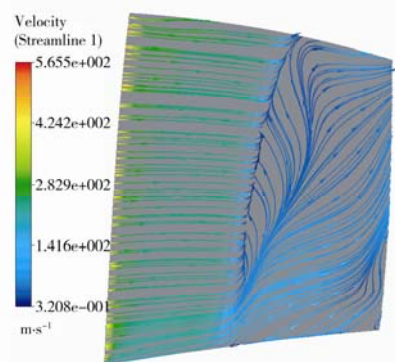


(b) 90% span

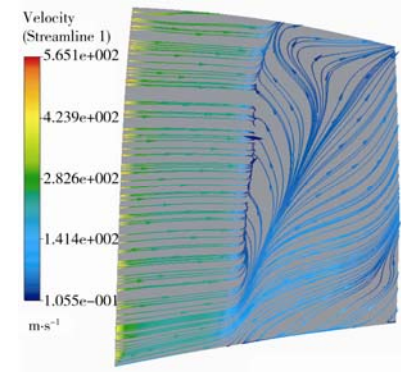
Fig.18 Blade loads of dry compressions at 50% and 90% spans under pressures 125534, 134534 and 135534 Pa



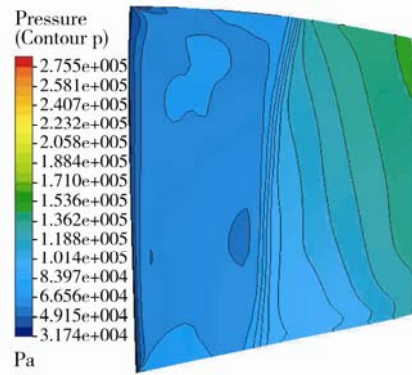
(a) Dry 134534 Pa



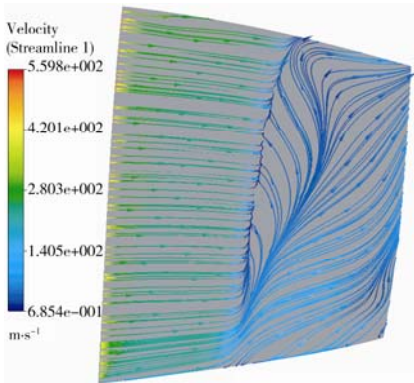
(b) Wet 180 g/s 5 μm 134534 Pa



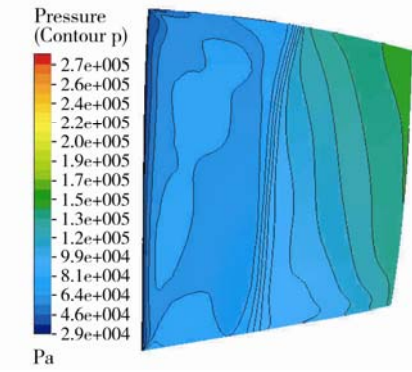
(c) Dry 135 534 Pa



(c) Dry 135 534 Pa



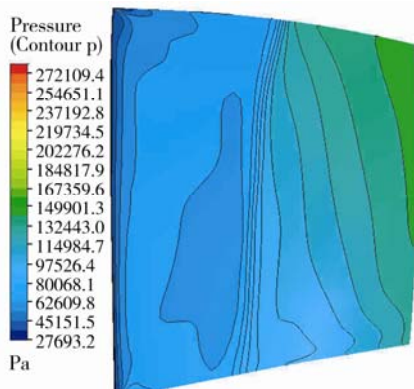
(d) Wet 180 g/s 5 μm 135 534 Pa



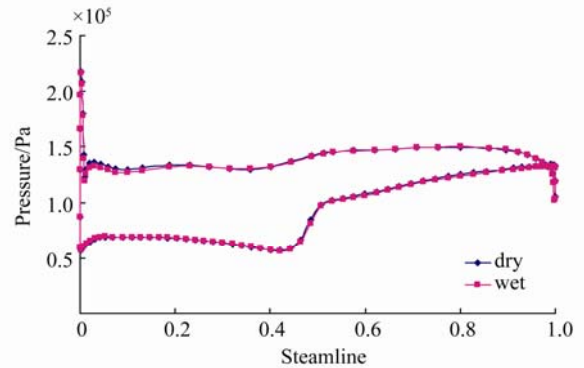
(d) Wet 180 g/s 5 μm 135 534 Pa

**Fig.19 Comparison of limiting streamlines on rotor suction surfaces between dry and wet compressions**

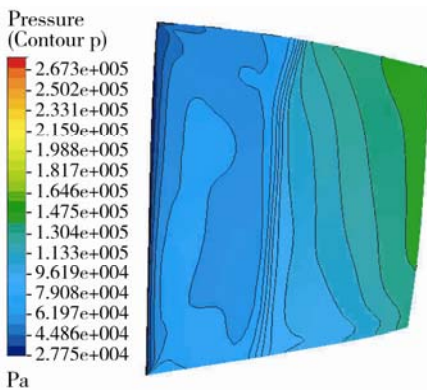
**Fig.20 Comparison of static pressures on rotor suction surfaces between dry and wet compressions**



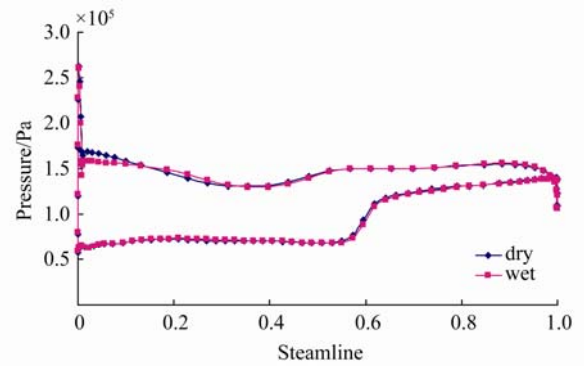
(a) Dry 134 534 Pa



(a) 50% span, 125 534 Pa



(b) Wet 180 g/s 5 μm 134 534 Pa



(b) 90% span, 125 534 Pa

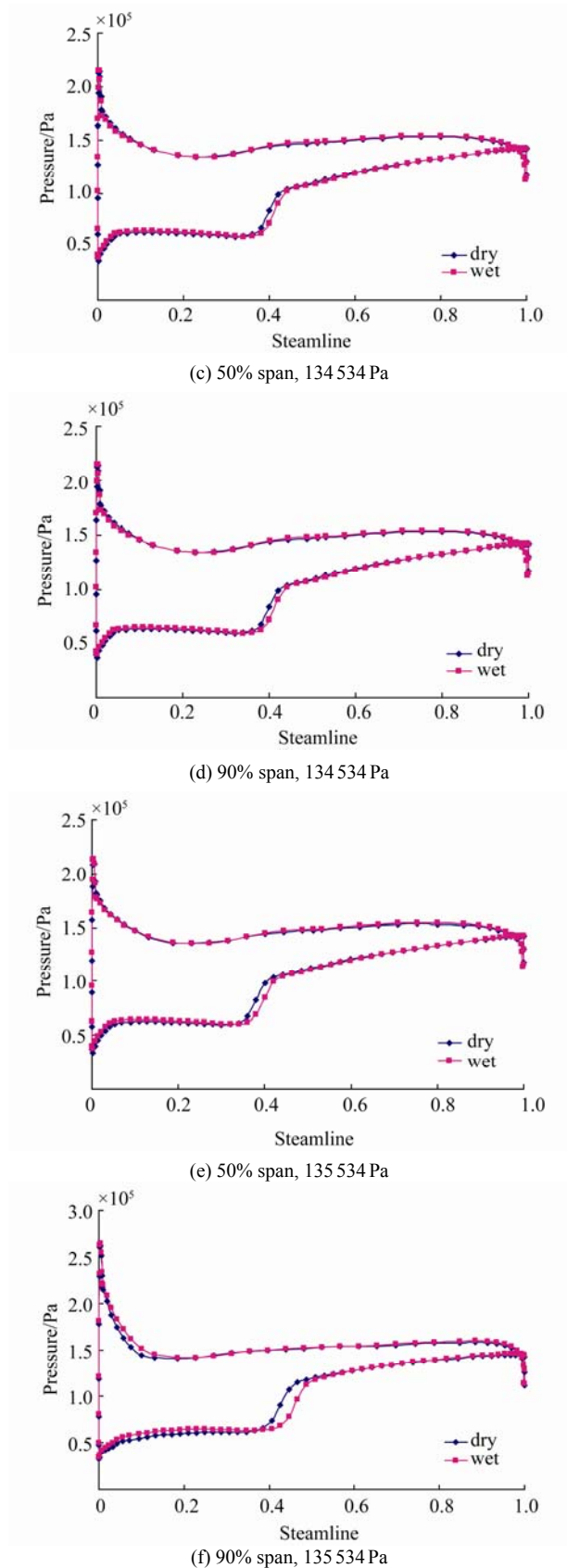
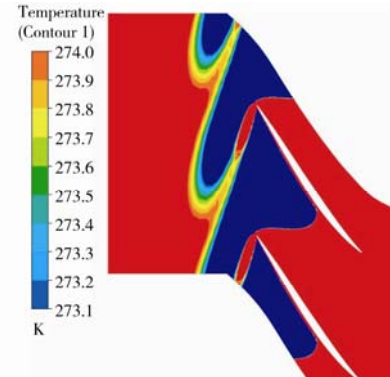


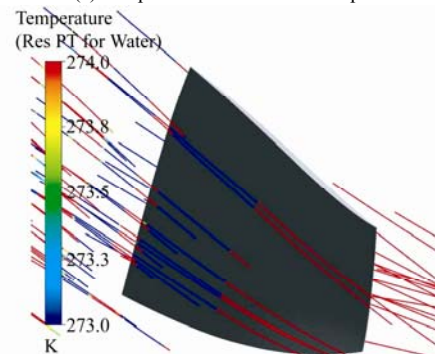
**Fig.21 Blade loads of wet compressions under 125 534, 134534 and 135 534 Pa, water flowrate 180 g/s, diameter 5 μm**

### 3.4 The problem of freezing with wet compression

For Rotor 37, because of the high velocity before the leading edge the static temperature will be lower than freezing point. It may be freezing, which is a troublesome problem. The blue area shows that the temperature is lower than freezing point. The particle may be freezing in this region in Fig.22(a). The Fig.22(b) shows the particle's static temperature changing and the blue part is below freezing point. If the particle collides with the blade in this blue part, the blade may be freezing which decreases the performance of compressor. But considered the particle inertia it should not collide with the suction side behind the leading edge.



(a) Temperature contour at 60% span



(b) Temperature of particle track

**Fig.22 Temperature contour and particle track at 60% span**

## 4 Conclusions

The wet compression is a complex flow process in the compressor, which includes the coupling process of continue phase and disperse phase and the phase changes. Based on the calculated data, Mach contours, streamlines and the loads of blade, we reach the conclusions as follows:

When the compressor runs near stall, the suited particle diameter and fogging rate can increase the inlet flow rate and pressure ratio and extend the range of stable operation. But the fogging also has some adverse effects that decrease the inlet flow rate and pressure ratio when the compressor runs at the design point.

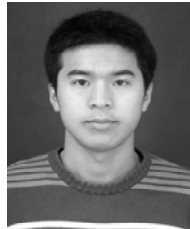
Generally, the fogging decreases the transonic compressor rotor efficiency in this paper. There should be an optimum particle diameter, which is 5 micron in this paper.

The main reason for extending the range of stable operation is the particle's momentum, which drives the low speed region to flow and improves the velocity of block region to make compressor run stably.

The evaporation has a function on the compressor rotor. However, the particle diameter is the main factor to extend the range of stable operation. There are some particularities for this phenomenon, namely, the inlet is atmosphere condition and the reason for stall is the leak eddy, which blocks the main passage.

## References

- Bhargava RK, Meher-Homji, CB, Chaker MA, Bianchi M, Melino F, Peretto A, Ingistov S (2005). Gas turbine fogging technology—a state of the art review: Part I—inlet evaporative fogging, analytical and experimental aspects. *Proceedings of ASME Turbo Expo*, Nevada, GT2005-68336.
- Bianchi M, Chaker M, Pascale AD, Peretto A, Spina PR (2007). CFD simulation of water injection in GT inlet duct using spray experimentally tuned data: nozzle spray simulation model and results for an application to a heavy-duty gas turbine. *Proceedings of ASME Turbo Expo*, GT-2007-27361.
- Bianchi M, Melino F, Peretto A, Spina PR, Ingistov S (2007). Influence of water droplet size and temperature on wet compression. *Proceedings of ASME Turbo Expo*, Montreal, GT2007-27458.
- Chaker M, Meher-Homji CB (2008). Gas turbine power augmentation-parametric study relating to fog droplet size and its influence on evaporative efficiency. *Proceedings of ASME Turbo Expo*, Berlin, GT-2008-51476.
- Chaker M, Meher-Homji CB, Mee III, TR (2003). Inlet fogging of gas turbine engines—experimental and analytical investigations on impaction pin fog nozzle behavior. *Proceedings of ASME Turbo Expo*, Atlanta, GT-2003-38801.
- Day IJ, Williams JC, Freeman C (2005). Rain ingestion in axial flow compressors at part speed. *Proceedings of ASME Turbo Expo*, Nevada, GT2005-68582.
- Fabbrizzi M, Cerretelli C, Medico FD, D'Orazio M (2009). An experimental investigation of a single stage wet gas centrifugal compressor. *Proceedings of ASME Turbo Expo*, Orlando, GT-2009-59548.
- Furukawa M, Inoue M, Saiki K, Yamada K (1998). The role of tip leakage vortex break down in compressor rotor aerodynamics. *Proceedings of ASME Turbo Expo*, 98-GT-239.
- Härtel C, Pfeiffer P (2003). Model analysis of high-fogging effects on the work of compression. *Proceedings of ASME Turbo Expo*, GT 2003-38117.
- Hofman W, Ballmann J (2002). Tip clearance vortex development and shock-vortex-interaction in a transonic axial compressor rotor. *Proceedings of AIAA*, Massachusetts, 2002-0083.
- Li Minghong, Zheng Qun. (2004). Wet compression system stability analysis: part I—wet compression Moore Greitzer transient model. *Proceedings of ASME Turbo Expo*, Vienna, GT-2004-54018.
- März J, Hah C, Neise W (2001). An experimental and numerical investigation into the mechanisms of rotating instability. *Proceedings of ASME Turbo Expo*, GT-0536.
- Moore RD (1978). Design and overall performance of four highly loaded, high-Speed inlet stages for an advanced high-pressure-ratio core compressor. NASA Technical Report, NASA-TP-1337.
- Shao Yan, Zheng Qun, Zhang Yinyong (2006). Numerical simulation of aerodynamic performances of wet compression compressor cascade. *Proceedings of ASME Turbo Expo*, Barcelona, GT-2006-91125.
- Shibata T, Takahashi Y, Hatamiya S (2008). Inlet air cooling with overspray applied to a two-stage centrifugal compressor. *Proceedings of ASME Turbo Expo*, Berlin, GT-2008-50893.
- Song Yanping, Chen Fu, Yang Jun, Wang, Zhongqi (2005). A numerical investigation of boundary layer suction in compound lean compressor cascades. *Proceedings of ASME Turbo Expo*, Nevada, GT2005-68441.
- Sun Lanxin, Zheng Qun (2008). The effects of wet compression on the separated flow in a compressor stage. *Proceedings of ASME Turbo Expo*, Berlin, GT-2008-50920.
- Sven-Jürgen H, Roland M, Wolfgang H (2009). Stability enhancement of a multistage compressor by air injection. *Proceedings of ASME Turbo Expo*, Orlando, GT2009-59868.
- Ulrichs E, Joos F (2006). Experimental investigations of the influence of water droplets in compressor cascades. *Proceedings of ASME Turbo Expo*, Barcelona, GT-2006-90411.
- Wang Yunhui, Liu Min, Sun Yufeng, Liu Ziheng (2003). The analysis of post-stall transients of compression system with wet compression. *Journal of Engineering for Thermal Energy and Power*, **18**(103), 67-70.
- Wang Yunhui, Wang Guoxue, Li Shuying, Sun Yufeng (2002). Analysis on effects of wet compression on surge margin of a small gas turbine. *Proceedings of ASME Turbo Expo*, IJPGC2002-26042.
- Zheng Qun, Li Minghong (2004). Wet compression system stability analysis: Part II—simulations and bifurcation analysis. *Proceedings of ASME Turbo Expo*, Vienna, GT-2004-54020.



**Huafeng Yang** was born in 1982. He finished his BS and MS at Harbin Engineering University. Now he is working in Aviation Institute of China, Shenyang 606.



**Qun Zheng** doctor of engineering, professor, and PhD supervisor of marine engineering. He finished his BS, MS and PhD at Harbin Engineering University. He has been working in the College of Power and Nuclear Energy Engineering of HEU after he got the bachelor degree. His research interests include aerodynamics and thermodynamics.



**Mingcong Luo** was born in 1986. He received the BS degree in Thermal Energy and Power Engineering from Harbin Engineering University and now he is studying for his PhD degree in Marine Engineering in this university. His research direction is analysis of system and general performance of the power equipments.